

Track-to-track association algorithm for passive multisensor system based on trajectory parameter

Mingyang Ma^{1,2}  | Dejiang Wang¹ | Tao Zhang¹ | He Sun¹

¹Key Laboratory of Airborne Optical Imaging and Measurement, Changchun Institute of Optics, Fine Mechanics and Physics, Chinese Academy of Sciences, Changchun, China

²University of Chinese Academy of Science, Beijing, China

Correspondence

Dejiang Wang, Key Laboratory of Airborne Optical Imaging and Measurement, Changchun Institute of Optics, Fine Mechanics and Physics, Chinese Academy of Sciences, Changchun 130033 China.
Email: wangdj04@ciomp.ac.cn

Funding information

Nation Natural Science Foundation of China, Grant/Award Numbers: 61627819, 61675202, 61727818, 61905240

Abstract

Asynchronous sampling and the ghost point are significant issues in the track-to-track association (TTTA) for passive multisensor system. A TTTA algorithm is proposed based on a trajectory parameter to address these issues. According to advantages in which the trajectory information can represent the target motion state and will not change with the sampling time, we turn the TTTA problem into the trajectory parameter matching problem. First, a TTTA model is established by the heading angle and the target velocity. Then, an estimation of target velocity that is suitable for asynchronous sampling is modelled using trajectory parameters from different sensors. Furthermore, to avoid the ghost point in the data association, we use only the bearing measurement of a single sensor to derive the trajectory parameters. Finally, an assignment method is adopted to determine the correspondence between different tracks. The simulation results demonstrate the effectiveness of the proposed method compared with competing algorithms.

1 | Introduction

Track-to-track association (TTTA) is a fundamental problem in the field of passive multisensor networks [1]. It determines whether two tracks from different sensors correspond to the same target [2]. It is the prerequisite for target tracking and location. For the TTTA problem, most previous work employs position components of local tracks to establish the association model [3]. However, the passive sensor can provide only bearing measurements, which are nonlinear functions of the target position. To acquire the target position and further determine the correspondence, the two-step (TS) method is widely adopted. It first estimates the target position using fundamental trigonometric identities and defines a cost function of the estimation and measurement. Then, the optimal correspondence is determined by a linear assignment algorithm [4].

In practice, two major problems affect the accuracy of the traditional TS algorithm in TTTA. The first problem is asynchronous sampling. The commonly suggested assumption in the TTTA problem is that each sensor works synchronously

and the data are transferred to the fusion centre at the same time [5]. However, in the real-world association system, sensors in the working scenario often have different sampling rates and sensors have different communication delays. The second problem is the ghost point, which is defined as incorrect association results [6]. This inherent problem is inherent in the cross-location principle that is commonly adopted by numerous data association models. The problem becomes more serious when the target number increases. In this sense, these two challenging problems lead to the performance degradation of traditional TTTA algorithms.

To overcome asynchronous sampling, many methods rearranged bearing measurements based on time alignment before TTTA [7,8]. To avoid the ghost point, an extra sensor is used to verify the correctness of the association result [9–11]. However, these approaches require the fusion centre to have a high sampling frequency and bring extra computation to the data association [12]. Recently, more attentions has been paid to bearing-only target motion analysis (TMA) [13]. This adopts a filtering method to improve the estimation accuracy of the target state and suppress the ghost point in the time dimension

[14]. For example, the pseudo-linear estimation (PLE) method [15] converts the nonlinear estimation model to a linear one through the cross-location principle and adopts the least-squares method to obtain the target state. Another general TMA uses the maximum-likelihood (ML) method [16]. In this technique, no approximation to the original nonlinear equations is needed as in the derivation of the PLE. Although, these methods are widely used to solve the TTTA problem, they are suitable for only a single target and are still challenging with asynchronous sampling.

We propose a novel TTTA algorithm based on trajectory parameter to overcome the problems of asynchronous sampling and the ghost point. Based on the advantage that the trajectory information can represent the motion state of the target and will not change with the sampling time [17], we turn the TTTA problem into the trajectory parameter matching problem. Under the assumption that the targets in the observation scenario have a constant velocity (CV), the mathematical model of TTTA is established by the heading angle and target velocity. Then, we associate the trajectory parameters from different sensors to estimate the velocity. Furthermore, a filtering method is provided to obtain the trajectory parameters by the bearing measurement from a single sensor. Finally, simulation results demonstrate that the proposed algorithm can achieve superior performance in terms of the probability of correct association (PCA).

2 | Problem formulation

In the distributed passive multisensor system, each sensor detects and tracks multiple moving targets and reports the tracks to the fusion centre independently. Then, the fusion centre finds the correspondence between different tracks based on the TTTA algorithm. The cost function of TTTA model is commonly established by errors between measurements and the real target position [18]. To solve this TTTA model, previous work commonly adopted the TS method, which includes target position estimation and optimal assignment. The accuracy of target position estimation directly affects the performance of TTTA. Assume that there are two passive sensors and two targets in the surveillance region. The location of each sensor $\{(x_{oi}, y_{oi})\} (i = 1, 2)$ is assumed to be known exactly. As shown in Figure 1, the measurement process is implemented in the global Cartesian coordinate system (GCCS). Let β_{j, n_i} denote measurement j from sensor i at sampling time n_i . $T_j (j = 1, 2)$ denote the real target. Each sensor i sends the measurements to the fusion centre. Then, the estimation position (x_{j, n_i}, y_{j, n_i}) of the target at time n_i can be calculated by:

$$\tan \beta_{j, n_i} = \frac{x_{j, n_i} - x_{oi}}{y_{j, n_i} - y_{oi}} \quad (1)$$

However, Formula (1) is efficient only in the synchronous sampling system, $t_{n1} = t_{n2}$. In practice, the sampling times of different sensors do not coincide. Figure 2 depicts a situation

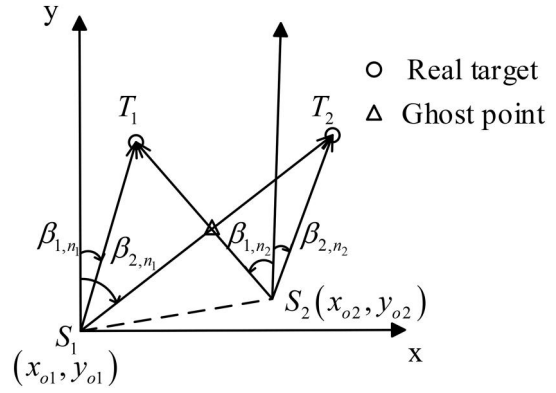


FIGURE 1 The estimation model of target position

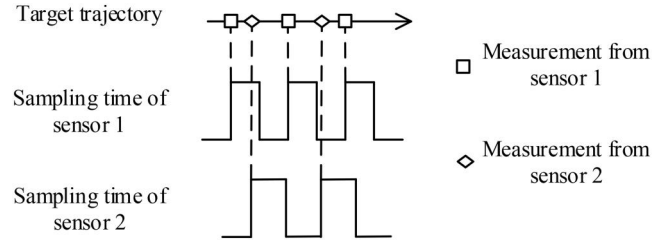


FIGURE 2 Example of asynchronous sampling of two sensors

in which the sampling time and sampling rate of two sensors are different. In this case, the target location estimated by Formula (1) will deviate from the real track.

Besides asynchronous sampling, the problem of ghost point affects the estimation accuracy. As shown in Figure 1, $\beta_{2, n1}$ and $\beta_{1, n2}$ do not correspond to the same target. However, according to Formula (1), a ghost point will be formed, which is marked by a triangle in Figure 1. This is the inherent problem in the cross-location principle and will be more serious with an increasing number of targets.

The problems of asynchronous sampling and ghost points directly affect the estimation accuracy and lead to a dramatic deterioration of the traditional TTTA algorithm. To overcome these problems, a TTTA model is established based on the trajectory parameters here.

3 | Proposed track-to-track association algorithm

The objective of the proposed algorithm is to turn the TTTA problem into a trajectory parameter matching problem. It is assumed that the motion of all targets follows the CV model in the GCCS. In this model, the heading angle and velocity are reliable trajectory parameters. Thus, a TTTA model is first established based on these trajectory parameters in this section. Then, to estimate the heading angle and target velocity, we propose a data association method and a filtering method, which are suitable for asynchronous sampling and can effectively avoid the ghost point.

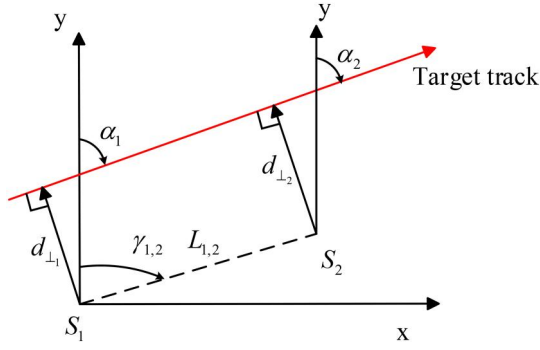


FIGURE 3 Target velocity estimation

$\alpha_1 = \alpha_2$. To estimate the target velocity, we focus on describing the relationship between two sets of trajectory parameters and the target velocity. According to the geometric relationship in Figure 3, the velocity can be estimated by:

$$V_{1,2}(t_{n_1}) = \frac{L_{1,2} \sin(\gamma_{1,2} - \alpha_1(t_{n_1}))}{d_{\perp 1}/V(t_{n_1}) - d_{\perp 2}/V(t_{n_2})} \quad (8)$$

The advantage of the proposed association method can be seen from Formula (8) and Figure 3. On the one hand, the target velocity estimation is modelled based on the geometric relationship between the target track and the relative location of two sensors, rather than the cross-location principle. The cross of two sensors' line of sight (LOS) is not needed in the velocity estimation. Therefore, the problem of the ghost point is directly avoided. On the other hand, α and d_{\perp}/V are the constant values that represent the target motion in the GCCS. They will not be affected by sampling time t_{n_i} . In other words, although the sampling time of different sensors is asynchronous, $t_{n_1} \neq t_{n_2}$, the heading angle and velocity estimated from different sensors are equal, which can be expressed as $\alpha(t_{n_1}) = \alpha(t_{n_2})$ and $V(t_{n_1}) = V(t_{n_2})$.

3.3 | Trajectory parameter filtering method

The proposed TTTA model consists of some trajectory parameters to be solved. To avoid the ghost point, these parameter sets should be obtained by each sensor independently rather than using the data association method. In this section, we represent a filtering method that is suitable for the single sensor observation. An overview of the passive sensor observing the target continuously in the GCCS is shown in Figure 4. The relationship between the trajectory parameters and bearing measurement is modelled by:

$$\cot(\alpha - \beta_n) = (t_n - t_{\perp})V/d_{\perp} \quad (9)$$

where β_n is the bearing measurement observed by the passive sensor at time t_n , which is defined as the angle between the y axis with LOS; t_{\perp} denotes the moment when the LOS of sensor is perpendicular to the target track.

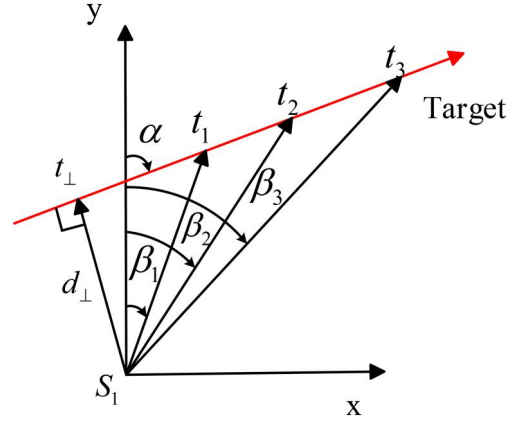


FIGURE 4 Schematic diagram of bearing-only observation

In practice, the measurement is usually corrupted with noise; that is, $\beta_n = \bar{\beta}_n + w_n$. $\bar{\beta}_n$ is the true bearing, w_n is the zero-mean, white Gaussian with standard deviation (STD) R_n . It is assumed that the noise measurement is irrelevant to the sampling time, $R = R_n$. Considering that each measurement has a different effect to the total noise, the calculation model of trajectory parameters could be established by the weighted least square principle. For the sequential associate time, we have:

$$f(\alpha, V/d_{\perp}, t_{\perp}) = \sum_{n=1}^W C_n [\cot(\alpha - \beta_n) - V(t_n - t_{\perp})/d_{\perp}]^2 \quad (10)$$

where $C_n = d_{\perp} \sin^2(\alpha - \beta_n)/(RV^2 \sin^2 \alpha)$ is a constant value. To simplify the operation, we define the pseudo-variate:

$$X = \left[t_{\perp} + \frac{d_{\perp}}{V} \cot \alpha \quad \frac{d_{\perp}}{V} - t_{\perp} \cot \alpha \quad \cot \alpha \right]^T \quad (11)$$

When $\frac{\partial f(\alpha, V/d_{\perp}, t_{\perp})}{\partial X} = 0$, the minimisation solution of $f(\alpha, V/d_{\perp}, t_{\perp})$ can be derived. Furthermore, the trajectory parameters can be obtained. The matrix equation of $\frac{\partial f}{\partial X} = 0$ can be expressed as:

$$A_n X = B_n \quad (12)$$

where:

$$A_n = \begin{bmatrix} \cos \beta_1 & \sin \beta_1 & t_1 \sin \beta_1 \\ \cos \beta_2 & \sin \beta_2 & t_2 \sin \beta_2 \\ M & M & M \\ \cos \beta_W & \sin \beta_W & t_W \sin \beta_W \end{bmatrix} \quad (13)$$

$$B_n = [t_1 \cos \beta_1 \quad t_2 \cos \beta_2 \quad \dots \quad t_W \cos \beta_W]^T \quad (14)$$

The noise of coefficient matrix A_n and data vector B_n is nonlinear. To obtain the precise solution, the measurement

noise should be separated. We retain the linear parts and omit items more than two orders by the Taylor series expansion. Thus, the solution of Formula (12) is transformed into a constrained least squares (CTLS) problem:

$$\begin{cases} \min_X \|u\|_F^2 \\ \text{s.t. } A_n X - B_n + \left(\sum_{i=1}^3 g_i x_i - g_4 \right) u = 0 \end{cases} \quad (15)$$

where $\|*\|_F^2$ is the Frobenius norm:

$$u = [\tilde{\beta}_1 \quad \tilde{\beta}_2 \quad \dots \quad \tilde{\beta}_W]^T \quad (16)$$

$$g_1 = \text{diag}\{\sin \beta_n\}_{W \times W} \quad (17)$$

$$g_2 = \text{diag}\{-\cos \beta_n\}_{W \times W} \quad (18)$$

$$g_3 = \text{diag}\{-t_n \sin \beta_n\}_{W \times W} \quad (19)$$

$$g_4 = \text{diag}\{t_n \sin \beta_n\}_{W \times W} \quad (20)$$

Minimising the noise u of the sequential sampling times, the trajectory parameters can be obtained. Moreover, the sensors can submit these parameter sets to the fusion centre for the TTTA.

Combing the matching model and the optimal estimation of the trajectory parameters, the proposed parametric TTTA model can be rewritten as:

$$E(\rho) = \min_{\rho_{j_1 \dots j_s}} \sum_{j_1=0}^{J_1} \dots \sum_{j_s=0}^{J_s} Q_{j_1 \dots j_s} \rho_{j_1 \dots j_s} + \min_X \sum_{i=1}^s \sum_{j_i=0}^{J_i} \|u_{j_i}\|_F^2 \quad (21)$$

where u_{j_i} is the measurement noise of target j_i from sensor i .

The proposed model in total consists of two parts. The first part is used to describe the similarity of the trajectory parameters between targets obtained by different sensors. The second part represents the trajectory parameters (velocity and heading angle) calculated from observation angles with measurement noise.

4 | Solution to the optimization model

The optimization model of Formula (21) is a mixed-integer nonlinear programming problem consisting of an optimal S-dimensional (S-D) assignment problem and a CTLS problem. The method for solving the S-D assignment problem has been deeply investigated using neural networks [19], genetic algorithms [20], and Lagrangian relaxation [21]. The method in a previous study [22] is used here to solve the problem owing to computational efficiency. The current work focuses on the solution and analysis of Formula (15).

Formula (15) is a quadratic minimisation problem that is subject to a quadratic constraint equation. A closed-form

solution to it may not exist. However, Coello et al. [23] demonstrated that the CTLS problem can be transformed into an unconstrained one over variable X . Consequently, the CTLS solution of Formula (15) can be obtained by minimising:

$$\begin{aligned} F(X) &= u^T u \\ &= \begin{bmatrix} X \\ -1 \end{bmatrix}^T [A_n \quad B_n]^T (G_x G_x^T)^{-1} [A_n \quad B_n] \begin{bmatrix} X \\ -1 \end{bmatrix} \end{aligned} \quad (22)$$

where $G_x = \sum_{i=1}^3 g_i X_i - g_4$. X_i is the i th column vector of X .

Many solution strategies exist to solve this optimization problem. A basic approach is the Newton method. However, the second partial derivative of $F(X)$ is difficult to calculate. To simplify the computation of the second partial derivative of $F(X)$, we adopt the BFGS (Broyden, Fletcher, Goldfarb and Shanno (BFGS) method, which is a popular quasi-Newton method widely used in many fields [24]. The pseudo-code of the BFGS to calculate the trajectory parameter is described in Table 1. The calculation of first partial derivative $\nabla F(X)$ is given in the Appendices.

Unlike the traditional approaches, the proposed TTTA algorithm does not need the interpolation of sampling time in advance and the estimation of the target position in data association. It includes two steps, which is similar to the framework of the traditional TTTA method. First, according to the filtering method, each sensor can derive the trajectory parameters for all of the detected target tracks, which include α , V/d_{\perp} and t_{\perp} . Then, the fusion centre associates the parameter sets submitted from different sensors to estimate the target and further determine the correspondence of different tracks. The flowchart of the proposed TTTA algorithm based on trajectory parameter is shown in Figure 5, in which it is assumed that there are two sensors and two targets in the scenario. The indexes of sensors are 1 and 2. The targets are expressed as i and j .

5 | Simulation and analysis

In this section, we design two simulation scenarios to illustrate the effectiveness of the proposed algorithm.

5.1 | A case of targets moving in constant velocity model

First, we consider a case of targets moving in CV model. As shown in Figure 6, there are 10 targets and three sensors in the simulation scenario. The trajectory parameters of targets are shown in Table 2. Sensors are located at $(-10 \text{ km}, 0 \text{ km})$, $(0 \text{ km}, 0 \text{ km})$ and $(10 \text{ km}, 0 \text{ km})$, respectively. The first sensor is assumed to be the fusion centre. In Figure 6, we have marked the starts, ends and indexes of the tracks. For each sensor, the measurement-to-track association is assumed known. The

TABLE 1 Pseudo-code of Broyden, Fletcher, Goldfarb and Shanno for trajectory parameter calculation

<p>Define $F(X) = u^T u$ and error factor τ. D^1, X are initialised to an identity matrix and unit vector, respectively. Initialise $k = 1$.</p> <p>Calculate $\nabla F(X^k)$ and $F(X^k)$, $k = k+1$</p> <p>DO WHILE($F(X^k) - F(X^{k-1}) > \tau$)</p> <p>Step 1) $X^k = X^{k-1} - D^{k-1} g^{k-1}$</p> <p>Step 2) $s = -D^{k-1} g^{k-1}$</p> <p>Step 3) $y = \nabla F(X^k) - \nabla F(X^{k-1})$</p> <p>Step 4) $D^k = \left(I - \frac{ys^T}{y^T s} \right) D^{k-1} \left(I - \frac{y^T s^T}{y^T s} \right) + \frac{ss^T}{y^T s}$</p> <p>Step 5) $k = k+1$</p> <p>REPEAT</p>
--

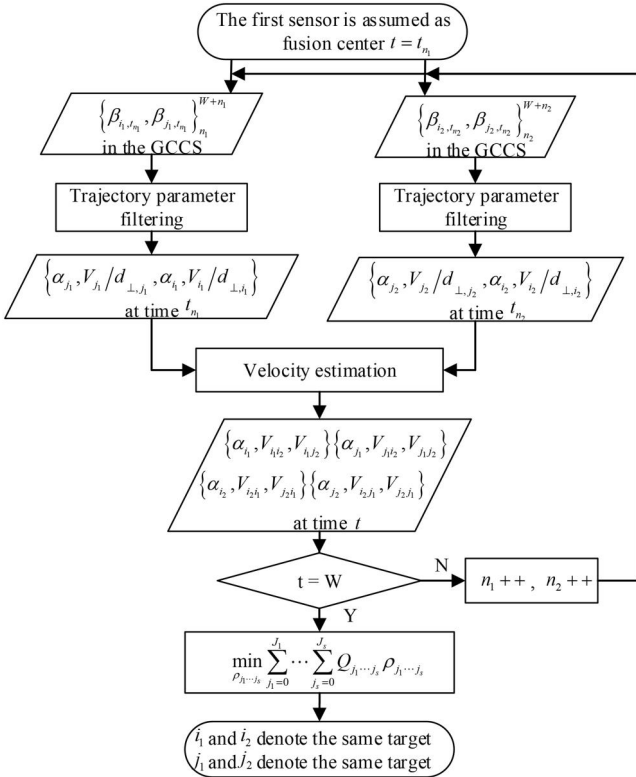


FIGURE 5 Flowchart of the proposed algorithm. GCCS, global Cartesian coordinate system

detection probability is set to $P_{d1} = P_{d2} = P_{d3} = 0.8$. The STD of bearing measurement noise is $R = 0.1$ degrees. In addition, we assume the STDs of measurement noise of three sensors are same. The sampling interval is 1 s, and 200 discrete time instants are used in the simulation.

$$P_{ca} = \frac{1}{K} \sum_{i=1}^K \frac{n_a^i}{n_{total}} \quad (23)$$

The association performance is evaluated by the PCA [25], which where K is the number of Monte-Carlo runs. n_{total} is the

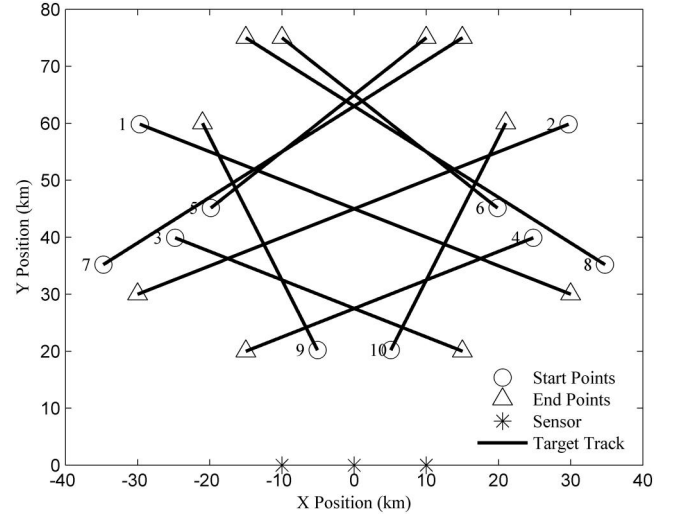


FIGURE 6 Simulation scenario 1

number of common targets observed by both three sensors. n_a^i is the number of targets with the correct association at the i th Monte-Carlo. Here, the correct association means that three local tracks come from the same target which is represented by $\rho_{j_1 j_2 j_3} = 1$. Experiment results are an average of 50 times Monte-Carlo simulation.

To demonstrate the advantage of the proposed algorithm, we compared the simulation results between the proposed algorithm, the classical TS algorithm with time alignment (TS-TA) [8], the TS algorithm with confirmation by third sensors [10], the PLE algorithm [15] and the ML algorithm [16].

The influence of the measurement noise on the performance of the proposed algorithm is first tested. To verify the adaptability of the algorithms to measurement noise, we appropriately alter the STD of measurement noise and keep other simulation parameters invariable. The STD of measurement noise R varies from 0.1 to 1 degrees. The association results are shown in Figure 7.

Figure 7 shows that the performance of the proposed algorithm remains stable and obviously outperforms other comparison algorithms. This demonstrates that the proposed filtering method can suppress the measurement noise

Target index	Initial state (km)	Heading angle (degrees)	Velocity (m/s)
1	(-30,60)	116.6	335.4
2	(30,60)	-116.6	335.4
3	(-25,40)	116.6	223.6
4	(25,40)	-116.6	223.6
5	(-20,45)	45.0	150.0
6	(20,45)	-45.0	150.0
7	(-35,35)	51.3	320.2
8	(35,35)	-51.3	320.2
9	(-5,20)	-20.6	215.4
10	(5,20)	20.6	215.4

TABLE 2 Trajectory parameters of targets in scenario 1

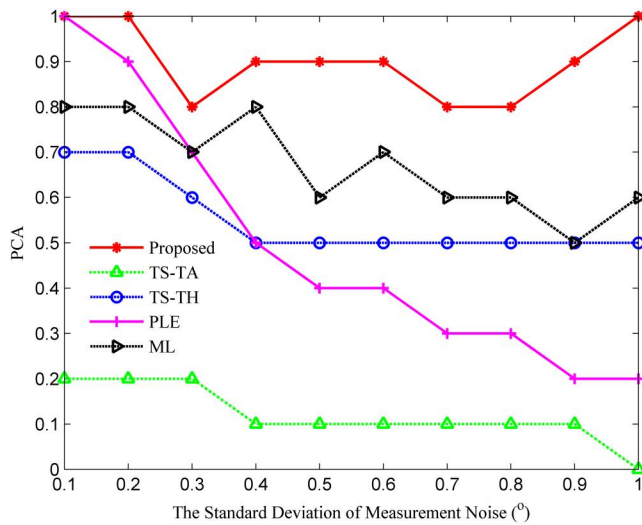


FIGURE 7 Performance of algorithms at different measurement noises for scenario 1. ML, maximum-likelihood; PLE, pseudo-linear estimation; TS-TA, two-step time alignment

effectively. When the measurement noise increases, the problem of the ghost point will be serious, which directly results in the decline of the performance of the TS algorithm. Because the PLE algorithm is a biased estimation, it has a maximum impact of measurement noise. The ML algorithm adopt the nonlinear method to solve the estimation problem. Thus, it has a better performance than PLE.

Second, we test the influence of distance bias δL between sensors on the performance of the proposed algorithm. It is assumed that the distance bias satisfies a Gaussian distribution with zero mean and the distance bias of any two sensors is same, described as $\delta L = \delta L_{1,2} = \delta L_{1,3} = \delta L_{2,3}$. The STD of δL varies from -1.5 to 1.5 km. The STD of measurement noise is kept at $R = 0.1^\circ$. The association results are shown in Figure 8.

Figure 8 shows that because all of the algorithms use the distance between two sensors, they are all sensitive to the distance bias. However, the proposed algorithm is better than other comparisons.

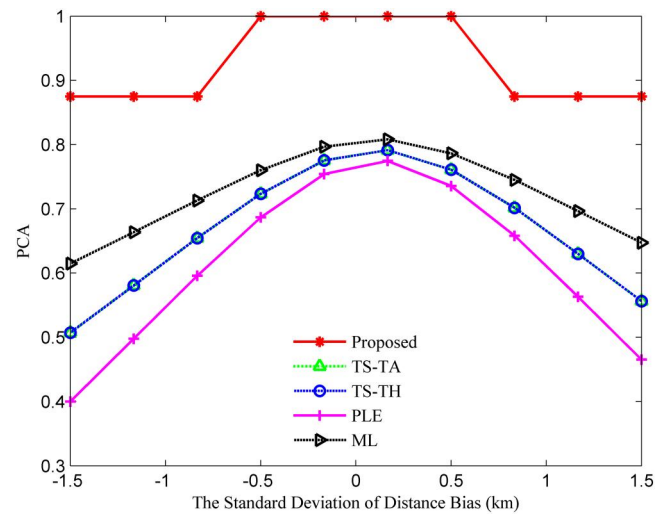


FIGURE 8 Performance of algorithms at different distance biases for scenario 1. ML, maximum-likelihood; PLE, pseudo-linear estimation; TS-TA, two-step time alignment

Third, we use the sampling delay to test the influence of asynchronous sampling on the performance of the proposed algorithm. Sampling delay $\delta T_{1,i}$ is defined as the delay between the fusion centre (sensor 1) and the other sensor i . It is assumed that $\delta T = \delta T_{1,2} = \delta T_{1,3}$. The δT varies from 0 to 50 s. Other simulation parameters are invariable. The association result is shown in Figure 9.

Figure 9 shows that the proposed algorithm remains stable with the increase in the sampling delay. Thus, it demonstrates that the proposed algorithm is adaptive to the asynchronous sampling. When sampling delay increases, the performance of the classical TS algorithm, PLE algorithm and ML algorithm declines dramatically. However, with the time alignment method, the TS-TA algorithm has better performance than the other comparison algorithms.

Finally, we analyse the influence of association time W , which is an important parameter in all of the cost functions of TTTA algorithms. The STD of measurement noise R is set to 0.1 degrees. The distance bias is kept at $\delta L = 0.5$ km. It is also

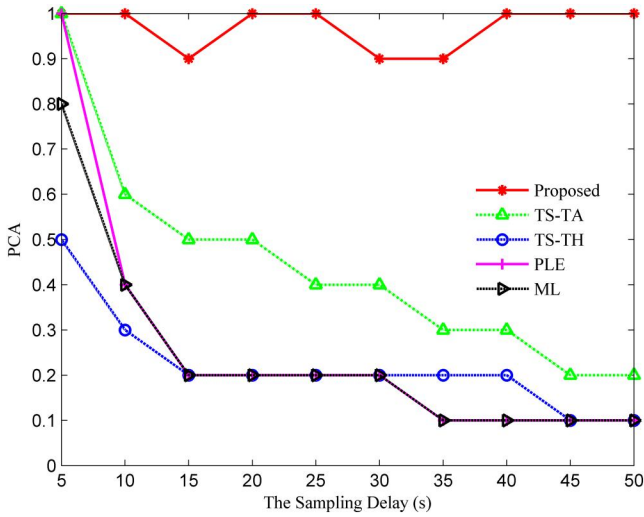


FIGURE 9 Performance of the algorithms in different sampling delays for scenario 1. ML, maximum-likelihood; PLE, pseudo-linear estimation; TS-TA, two-step time alignment

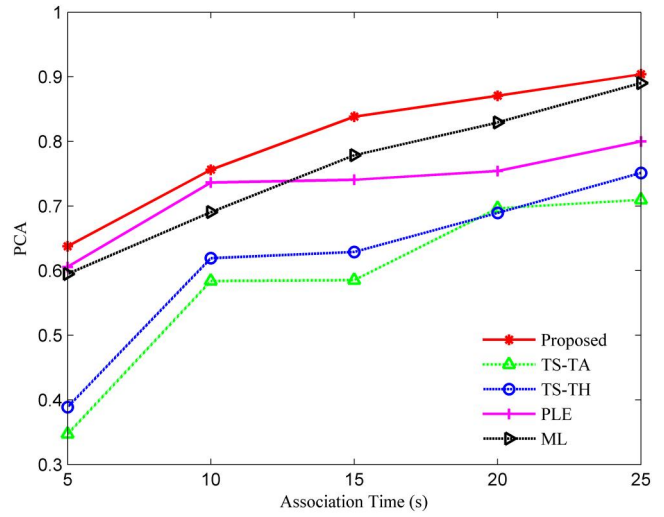


FIGURE 10 Performance of algorithms in different association times for scenario 1. ML, maximum-likelihood; PLE, pseudo-linear estimation; TS-TA, two-step time alignment

assumed that there is no sampling delay in TTTA. Association time W varies from 5 to 25 s. The simulation results are shown in Figure 10.

With the increase in association time, more valid measurements are available. They help to improve the performance of all algorithms gradually. For the traditional TS algorithm, too little time is equivalent to inadequate data, which fail to reveal the dominant similarity of different tracks. Because the time alignment is adopted before TTTA, the TS-TA has improved the performance of the TS algorithm. The estimation of PLE algorithm is biased. Thus, when the association time is greater than 10, the PCA increases slowly. Because the proposed algorithm can obtain precise trajectory parameters in a short time, it has a higher PCA than other algorithms.

These simulation results have shown that the proposed algorithm has a better performance than traditional TTTA algorithms. Moreover, they demonstrate that the proposed algorithm can fit the situation of asynchronous sampling and effectively avoid the ghost point.

In the proposed TTTA model, we assume that targets satisfy the CV model in the observation scenario. In fact, the target velocity is changeable. Thus, another simulation is used to illustrate the adaptation of the proposed algorithm for maneuvering targets. The tracks of all targets are shown in Figure 11. The initial states and velocities are same as in scenario 1. The detailed trajectory parameters of targets are shown in Table 3. The sampling interval is 1 s and 100 discrete time instants are used in the simulation. In the first 50 s, targets move with a constant acceleration. At 50 s, the acceleration directions change abruptly and remain stable until the end of the simulation. Hence, the heading angles and velocities change over the sampling time.

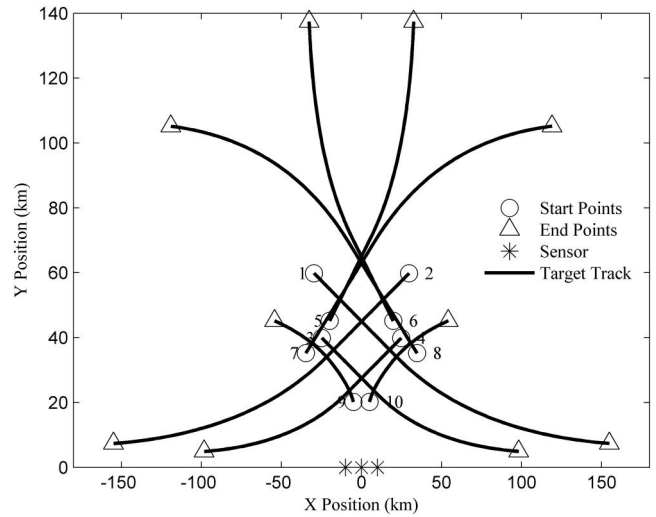


FIGURE 11 Simulation scenario 2

Figures 12–15 illustrate the PCAs of all algorithms via different measurement noise, distance biases, sampling delays and association times, respectively. The sets of simulation parameters and comparison algorithms are same as in scenario 1.

Figure 12 indicates that with small measurement noise, the competing algorithms achieve well. When the noise is serious, the association performances given by the comparison algorithms experience severe degradation. However, with the increase in the STD of measurement noise, the proposed algorithm remains stable. Figures 13 and 14 show that the PCAs of all algorithms are no more than 50%. When the targets are maneuvered, the proposed algorithm and comparison algorithms are sensitive to the distance bias and sampling delay. Figures 12 and 14 demonstrate that when target

Target index	Initial state (km)	Acceleration in 1–50 s (m/s^2)	Acceleration in 50–100 s (m/s^2)
1	(-30,60)	(30,-15)	(30,-15)
2	(30,60)	(-30,-15)	(-30,15)
3	(-25,40)	(20,-10)	(20,10)
4	(25,40)	(-20,-10)	(-20,10)
5	(-20,45)	(15,15)	(-15,15)
6	(20,45)	(-15,15)	(15,15)
7	(-35,35)	(25,20)	(25,-20)
8	(35,35)	(-25,20)	(-20,-20)
9	(-5,20)	(-8,2)	(-8,-2)
10	(5,20)	(-8,2)	(-8,-2)

TABLE 3 Trajectory parameters of targets in scenario 2

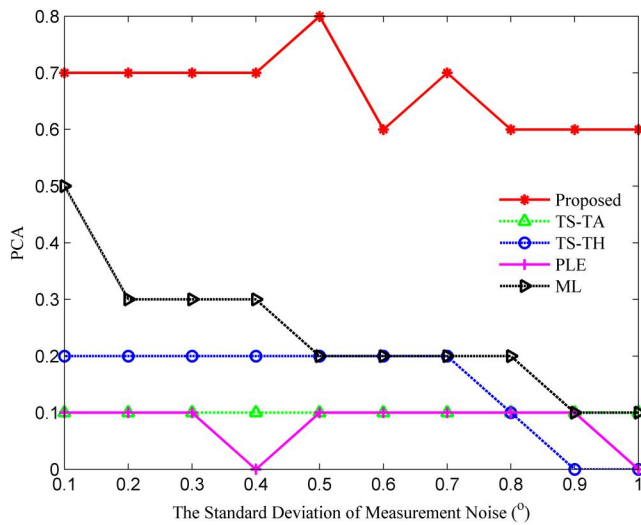


FIGURE 12 Performance of algorithms with different measurement noise for scenario 2. ML, maximum-likelihood; PLE, pseudo-linear estimation; TS-TA, two-step time alignment

maneuver occurs, the performances of the proposed algorithm with different measurement noise, distance biases and sampling delays are similar to the situation of targets with the CV model.

Figure 15 shows that with an increase in the association time, the proposed algorithm becomes more accurate to determine the correspondence between different targets, whereas the association results of the comparison algorithms degenerate rapidly. Figure 15 also shows that when $W > 35$, the PCA of the proposed algorithm reduces gradually. This simulation result demonstrates that the association time has a significant effect on association results for all of the algorithms when the target maneuver occurs. This is because the competing algorithms need to estimate the targets states before determining the correspondence. Because the association time is small, although targets are maneuvered, the states will not obviously change. Thus, the target states can be estimated exactly. With the increase in association time, the estimation

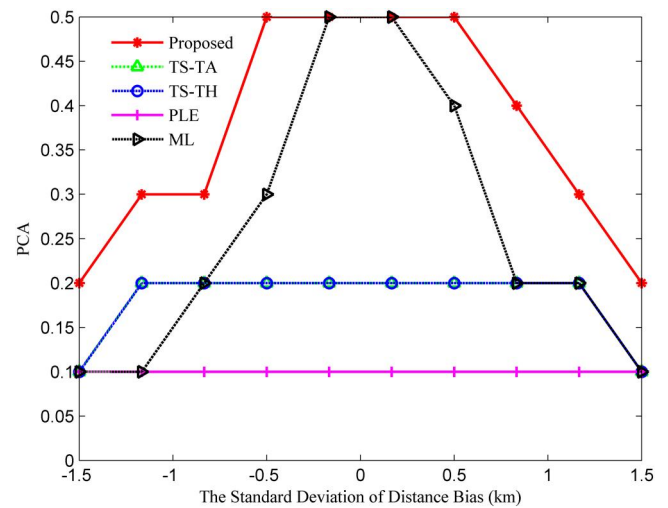


FIGURE 13 Performance of algorithms with different distance biases for scenario 2. ML, maximum-likelihood; PLE, pseudo-linear estimation; TS-TA, two-step time alignment

accuracy degenerates rapidly and the PCA declines. However, within a short sampling time, the changes in heading angles and velocities of targets are not obvious. Because the proposed TTTA model uses trajectory parameters, the PCA of the proposed algorithm is higher than for other algorithms. However, if the association time is too short, the information obtained by sensors is unavailable. The proposed algorithm cannot determine the correspondence. In addition, when the association time is too long, the trajectory parameters of the same target in these times are different. The proposed TTTA algorithm also cannot acquire good performance. Therefore, the trajectory parameters can be used to solve the TTTA problem in a certain association time when the targets are maneuvered.

These simulation results demonstrate that when the targets are maneuvered, the proposed algorithm still produces good association results and outperforms other competing algorithms. Certainly, it needs a suitable association time.

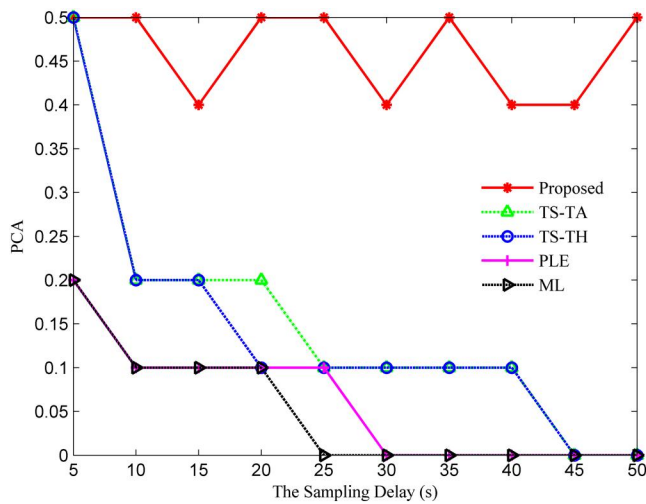


FIGURE 14 Performance of algorithms with different sampling delays for scenario 2. ML, maximum-likelihood; PLE, pseudo-linear estimation; TS-TA, two-step time alignment

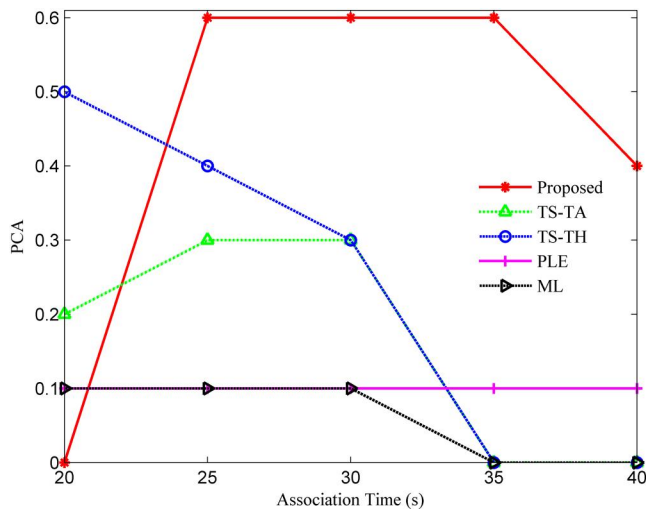


FIGURE 15 Performance of algorithms with different association times for scenario 2. ML, maximum-likelihood; PLE, pseudo-linear estimation; TS-TA, two-step time alignment

6 | Conclusion

To deal with the problems of asynchronous sampling and the ghost point in a passive multisensor system, a TTTA algorithm based on trajectory parameters is investigated. According to the heading angle and target velocity, a cost function is established to evaluate the similarity of different tracks from each sensor. Specifically, to fit asynchronous sampling, a velocity estimation method is designed by associating the trajectory parameters from different sensors. Finally, to obtain the trajectory parameters and avoid the ghost point, a filtering method is provided that is suitable for the single sensor observation. Numerical simulations are performed to demonstrate the effectiveness of the proposed TTTA model. The superiority has been illustrated and discussed

for four aspects: measurement noise, distance bias, sampling delay and association time.

ACKNOWLEDGEMENT

This work is supported by the Nation Natural Science Foundation of China (Nos. 61675202, 61627819, 61727818, and 61905240).

CONFLICT OF INTEREST

There are no conflicts of interest to declare.

ORCID

Mingyang Ma  <https://orcid.org/0000-0001-8795-4058>

REFERENCES

1. Qi, L., et al.: Anti-bias track-track association algorithm based on distance detection. *IET Radar Sonar Nav.* 11(2), 269–276 (2017)
2. Klein, I., Bar-Shalom, Y.: Tracking with asynchronous passive multisensor systems. *IEEE Trans. Aerosp. Electron. Syst.* 52(4), 1769–1775 (2016)
3. Li, Z., Zhang, W., You, H.: An adaptive threshold of two-stage data correlation algorithm for three-passive-sensor location system. *IEEE International Symposium on Systems and Control in Aeronautics and Astronautics.* Harbin, China (2006)
4. Pei-yih, T., Ronald, A.: Multitarget motion analysis in a DSN. *IEEE Trans. Syst. Man Cyber.* 21(5), 1125–1139 (1991)
5. Zhu, H., Han, C., Han, H.: Asynchronous track-to-track association method in distributed multi-sensor information fusion System. *Control Theory Appl.* 21(3), 453–456 (2004)
6. Bar-Shalom, Y., Li, X.R.: Multitarget-Multisensor tracking: principles and techniques. *IEEE control systems.* YBS, Storrs (1995)
7. Klein, I., Lipman, Y., Bar-Shalom, Y.: Asynchronous passive multisensor system observability with unknown sensor position. *IEEE Trans. Aerosp. Electron. Syst.* 54(1), 369–375 (2018)
8. Yu, Y., et al.: A sequential two-stage track-to-track association method in asynchronous bearings-only sensor networks for aerial targets surveillance. *Sensors.* 19, 1–20 (2019)
9. Musicki, D.: Multi-target tracking using multiple passive bearings-only asynchronous sensors. *IEEE Trans. Aerosp. Electron. Syst.* 41(3), 1151–1160 (2008)
10. Braca, P., et al.: Distributed information fusion in multistatic sensor networks for underwater surveillance. *IEEE Sensor J.* 16(11), 4005–4014 (2016)
11. Ouyang, C., Ji, H.: Modified cost function for passive sensor data association. *Electron Lett.* 47(6) 383–385 (2011)
12. Heist, S., et al.: GOBO projection for 3D measurements at highest frame rates: a performance analysis. *Light Sci. Appl.* 7(71), 1–3 (2018)
13. Sathyan, T., Sinha, A.: A two-stage assignment-based algorithm for asynchronous multisensor bearings-only tracking. *IEEE Trans. Aerosp. Electron. Syst.* 47(3), 2153–2168 (2011)
14. Talebi, H., Afshin-Hemmatyar, A.M.: Asynchronous track-to-track fusion by direct estimation of time of sample in sensor networks. *IEEE Sensors Journal.* 14(1), 210–217 (2014)
15. Nguyen, N., Dogancay, K.: Improved pseudolinear kalman filter algorithms for bearings-only target tracking. *IEEE Trans. Signal Process.* 65(23), 6119–6134 (2017)
16. Kirubarajan, T., Bar-Shalom, Lerro, D.: Bearings-only tracking of maneuvering targets using a batch-recursive estimator. *IEEE Trans. Aerosp. Electron. Syst.* 37(3), 770–780 (2001)
17. Dias, J., Marques, P.: Multiple moving target detection and trajectory estimation using a single SAR sensor. *IEEE Trans. Aerosp. Electron. Syst.* 39(2), 604–623 (2003)
18. Aziz, A.M.: A joint possibilistic data association technique for tracking multiple targets in a cluttered environment. *Inf. Sci.* 280, 239–260 (2014)
19. Leung, H.: Neural network data association with application to multiple-target tracking. *Opt. Eng.* 35(693), 1–10 (1996)

20. Carrier, J.Y., et al.: Genetic algorithm for multiple-target-tracking data association. *Aerosp. Def. Sens. Simul. Controls.* 2739, 180–190 (1996)
21. Poore, B., Robertson, A.J.A.J., III: A new Lagrangian relaxation based algorithm for a class of multidimensional assignment problems. *Comput. Optim. Appl.* 8, 129–150 (1997)
22. Der, S., et al.: 'A generalized S-D assignment algorithm for multisensory-multitarget state estimation'. *IEEE Trans. Aerosp. Electron. Syst.* 33(2), 523–538 (1997)
23. Coello, C.A., Pulido, G.T., Lechuga, M.S.: Handling multiple objectives with particle swarm optimization. *IEEE Trans. Evol. Comput.* 8(3), 256–279 (2004)
24. Povalej, Z.: Quasi-Newton's method for multiobjective optimization. *J. Comput. Appl. Math.* 255, 765–777 (2004)
25. Zhu, H., Wang, W., Wang, C.: Robust track-to-track association in the presence of sensor biases and missed detections. *Inf. Fusion.* 27, 33–40 (2016)

How to cite this article: Ma M, Wang D, Zhang T, Sun H. Track-to-track association algorithm for passive multisensor system based on trajectory parameter. *IET Radar Sonar Navig.* 2021;15:348–358. <https://doi.org/10.1049/rsn2.12040>

APPENDICES

Remark 1 $g(X) = X^T A X$. $\nabla g(X) = (A^T + A)X$

Remark 2 $\nabla g(X)^{-1} = -g(X)^{-1} \nabla g(X) g(X)^{-1}$

According to the two remarks, we can derive the $\nabla F(X)$. First, we define $g(X) = G_x G_x^T$

$$\begin{aligned} F(X) &= u^T u \\ &= \begin{bmatrix} X \\ -1 \end{bmatrix}^T [A_n \quad B_n]^T [g(X)]^{-1} [A_n \quad B_n] \begin{bmatrix} X \\ -1 \end{bmatrix} \end{aligned}$$

$$\begin{aligned} \nabla F(X) &= 2[A_n \quad B_n]^T [g(X)]^{-1} (A_n X - B_n) \\ &\quad - \begin{bmatrix} X \\ -1 \end{bmatrix}^T [A_n \quad B_n]^T \nabla g(X)^{-1} [A_n \quad B_n] \begin{bmatrix} X \\ -1 \end{bmatrix} \\ &= 2C_1 (A_n - C_2)^T \end{aligned}$$

where $C_2 = [G_x g_1^T C_1^T \quad G_x g_2^T C_1^T \quad G_x g_3^T C_1^T]$,

$$C_1^T = (G_x G_x^T)^{-1} (A X - B)$$